Research Article

Journal of Labelled Compounds and Radiopharmaceuticals

Received 8 December 2009, Revised 26 July 2010, Accepted 12 September 2010 Published online 30 November 2010 in Wiley Online Library

(wileyonlinelibrary.com) DOI: 10.1002/jlcr.1841

Synthesis and biological evaluation of ^{125}I/^{123}I-labelled analogues of citalopram and escitalopram as potential radioligands for imaging of the serotonin transporter

Jacob Madsen,[a*†] Betina Elfving,[b†] Vibe G. Frokjaer,[b] Birgitte R. Kornum,[b] Gerda Thomsen,[b] Lars Martiny,[c] and Gitte M. Knudsen[b]

Two novel radioligands for the serotonin transporter (SERT), [^{125}I]{3-[5-iodo-1-(4-fluorophenyl)-1,3-dihydroisobenzofuran-1-yl]-propyl}-dimethylamine ([^{125}I]-2) and *S*-[^{125}I]{3-[5-iodo-1-(4-fluorophenyl)-1,3-dihydroisobenzofuran-1-yl]-propyl}-dimethylamine ([^{125}I]-(*S*)-2) were synthesized in a Br/^{125}I exchange reaction. Binding experiments in rats yielded K_d values of 0.7 ± 0.06 and 0.52 ± 0.02 nM for [^{125}I]-2 and [^{125}I]-(*S*)-2, respectively. One hour after intravenous injection of [^{125}I]-2, 0.34% of the injected dose had accumulated in the brain. The highest hypothalamus-to-cerebellum ratio was reached 2 h after injection of [^{125}I]-(*S*)-2 and amounted to 2.4. Pre-treatment experiments with paroxetine resulted in effective reduction of the target-to-cerebellum ratios.

The corresponding iodine-123 labelled compound *S*-[^{123}I]{3-[5-Iodo-1-(4-fluorophenyl)-1,3-dihydroisobenzofuran-1-yl]-propyl}-dimethylamine [^{123}I]-*S*-2 was investigated in a pig single photon emission computed tomography (SPECT) study. Between 60 and 110 min after IV injection, the midbrain-to-cerebellum ratio was 1.2. However, the uptake did not differ between high-density and medium-density regions questioning the feasibility of the radioligand in imaging cortical SERT distribution *in vivo*.

These data suggest that the iodine-labelled derivatives of citalopram and escitalopram are not superior to another SPECT tracer for the SERT, namely [^{123}I]ADAM.

Keywords: serotonin transporter; escitalopram; SPECT; iodine labelling

Introduction

Positron emission tomography (PET) and single photon emission computed tomography (SPECT) are non-invasive techniques, which can be applied for *in vivo* investigations of biological processes in humans using appropriate radioligands.[1] Radioligands are labelled with radionuclides such as ^{11}C ($t_{1/2}$ = 20.4 min) or ^{18}F ($t_{1/2}$ = 109 min) for PET and ^{99m}Tc ($t_{1/2}$ = 6.0 h) or ^{123}I ($t_{1/2}$ = 13.1 h) for SPECT. The advantages of SPECT are first of all lower costs and the more facile handling of often longer lived SPECT radioligands, whereas PET is a quantitative method and the use of radioligands labelled with short-lived isotopes allow multiple investigations in the same subject on the same day.

The serotonin transporter (SERT) is believed to play a central role in mental disorders arising from disturbances in the serotonin system.[2] There are now several PET-radioligands available for imaging of the SERT in the living human brain, especially the diarylsulfides [^{11}C]DASB,[3,4] [^{11}C]MADAM,[5,6] and more recently [^{11}C]HOMADAM.[7,8] For SPECT imaging, iodinated diarylsulfides such as [^{123}I]ODAM, [^{123}I]IDAM and [^{123}I]ADAM have all been suggested as candidates for visualization of the SERT *in vivo*.[9–11] Within this series of compounds, [^{123}I]ADAM is the most promising candidate as a SPECT radioligand and has been evaluated in humans.[12–14] So far, [^{123}I]ADAM remains the only available SPECT radioligand for human studies. However, robust quantification of cerebral SERT requires a 120-min data acquisition and another potential disadvantage with this radioligand is the presence of a lipophilic metabolite seen in some subjects.[14]

In this paper, we report the radiolabelling and initial biological studies of iodinated derivatives of the selective serotonin reuptake inhibitors (SSRIs), citalopram and escitalopram. The novel radioligands [^{125}I]{3-[5-iodo-1-(4-fluorophenyl)-1,3-dihydroisobenzofuran-1-yl]-propyl}-dimethylamine (**[^{125}I]-2**) and

[a]*PET and Cyclotron Unit 3982, Copenhagen University Hospital, Blegdamsvej 9, 2100 Copenhagen Ø, Denmark*

[b]*Neurobiology Research Unit 9201, Copenhagen University Hospital, Blegdamsvej 9, 2100 Copenhagen Ø, Denmark*

[c]*Radiation Research Division, Risø DTU, Frederiksborgvej 399, 4000 Roskilde, Denmark*

**Correspondence to: Jacob Madsen, PET and Cyclotron Unit 3982, Copenhagen University Hospital, Blegdamsvej 9, 2100 Copenhagen Ø, Denmark. E-mail: jacob.madsen@rh.regionh.dk*

†*B. E. and J. M. have contributed equally to this work.*

S-[^{125}I]{3-[5-iodo-1-(4-fluorophenyl)-1,3-dihydroisobenzofuran-1-yl]-propyl}-dimethylamine ([**^{125}I]-(*S*)-2**) were investigated in *in vitro* and *ex vivo* assays. *S*-[^{123}I]{3-[5-Iodo-1-(4-fluorophenyl)-1,3-dihydroisobenzofuran-1-yl]-propyl}-dimethylamine **([^{123}I]-(*S*)-2)** was investigated for its potential use as radioligand for *in vivo* imaging of the SERT in the human brain using SPECT.

Materials and methods

No-carrier-added [^{125}I]sodium iodide solution (2 Ci/μmol) was purchased from Amersham Biosciences. Paroxetine hydrochloride was purchased from Smith-Kline Beecham, West Sussex UK. Male Sprague–Dawley rats weighing 206–396 g were used for the biological studies (M&B, Denmark). HPLC was performed on a Merck Hitachi fitted with in-line radio detection. Log *P* values were calculated with QikProp. {3-[5-bromo-1-(4-fluorophenyl)-1,3-dihydroisobenzofuran-1-yl]-propyl}-dimethylamine (**1**), *S*-{3-[5-bromo-1-(4-fluorophenyl)-1,3-dihydroisobenzofuran-1-yl]-propyl}-dimethylamine (***S*-1**) and {3-[5-iodo-1-(4-fluorophenyl)-1,3-dihydroisobenzofuran-1-yl]-propyl}-dimethylamine (**2**) were gifts from H. Lundbeck A/S, Copenhagen, Denmark. **[^{123}I]-(*S*)-2** was prepared by MAP Medical, Finland, from the stannylated precursor, (S)-{3-[(4-fluorophenyl)-5-tributylstannyl-1,3-dihydroisobenzofuran-1-yl]-propyl}-dimethylamine.[15]

Radiosynthesis of [^{125}I]-2 and [^{125}I]-(*S*)-2

To a 1-ml vial charged with **1** (1.6 mg, 4.2 μmol), citric acid (5.3 mg, 27.6 μmol), 2,5-dihydroxybenzoic acid (3.9 mg, 25.3 μmol), isoascorbic acid (3.6 mg, 20.4 mol) and $CuSO_4$ (0.2 ml, 1 mg/ml) was added acidic acid (0.2 ml, 1 M) and [^{125}I]sodium iodide (5 mCi). The vial was sealed and heated to 140°C for 2 h. After cooling to room temperature, the mixture was loaded on a Seppak Plus C_{18} cartridge (Waters). The cartridge was flushed with H_2O (2 ml) and the radioactive material was eluted with 70% CH_3CN (2 ml). The eluted material was evaporated to approximately 300 μl and diluted with 200 μl HPLC eluent. The mixture was split into two portions before purification. HPLC purification was performed on an analytical column (RP, OdDMeSi, 5 μm, 120 Å, 4.6 × 250 mm). HPLC eluent A: 0.1% TFA/10% CH_3CH and B: 0.1% TFA/90% CH_3CN were used. From 0–40 min, the eluent B was linearly increased from 25 to 40% with a 1-ml/min flow rate. The purified product, **[^{125}I]-2**, was analysed on a second HPLC system using an analytical column as above. The solvents A: 0.1% TFA/10% CH_3CH and B: 0.1% TFA/90% CH_3CN were used. From 0–30 min, solvent B was increased from 40 to 60%.

Applying the above procedure **[^{125}I]-*S*-2** was prepared using ***S*-1** as the starting material.

In vitro binding studies

Saturation binding studies were performed with rat brain homogenates of cerebrum ($n = 3$) according to a previous published procedure[16] and the K_d values were determined at 37°C.[17]

Ex vivo binding studies

Three rats per time point were used for *ex vivo* brain distribution studies. All animal experiments were carried out in accordance with the European Communities Council Resolves of 24th November 1986 (86/609/ECC) and approved by the Danish Animal Research Inspectorate (Journal number 2003/561–745).

The radioligand **[^{125}I]-2** was injected in the tail vein and the rats were decapitated 1, 2, 3, 4 and 6 h later. Rats injected with **[^{125}I]-(*S*)-2** were decapitated after 2 h. In all cases, the brains were quickly removed and dissected on an ice-cold tile. Eight brain regions (olfactory tubercles, hypothalamus, cerebellum, hippocampus, corpus striatum, thalamus, pre-frontal cortex and remaining cortex) were dissected, weighted and the accumulated radioactivity was counted. Paroxetine (3 mg/kg) was used in competitive binding studies. The region of interest (ROI)-to-cerebellum ratios were determined as [(ROI(cpm)/ROI(g))/(cerebellum(cpm)/cerebellum(g))]. The percent dose per gram brain tissue (% dose/g) was calcutated as [(ROI(cpm)/g ROI tissue)/total injected dose] for each brain region.

SPECT study

A Landrace pig, 33.5 kg, was used for the SPECT scan. The pig was sedated with an i.m. injection of midazolam (0.1 mg/kg). After 10–15 min, full anaesthesia was induced with 0.15 ml/kg i.m. of a mixture of Midazolam and Zoletil 50 vet. (Virbac Animal Health, France: 125 mg tiletamin and 125 mg zolazepam in a total volume of 8 ml Midazolam (1 mg/ml)) and maintained during the whole procedure using propofol (10 mg/ml, 51 ml/h). The pig was intubated and kept on a respiration rate of 12 ml/min. Arterial and venous catheters were inserted in the femoral artery and vein, and used for injection of **[^{123}I]-*S*-2**, saline and for taking blood samples. A saturation monitor on the tail monitored oxygen saturation and heart rate, and blood gases and electrolytes in arterial blood were measured with an ABL Blood Gas analyzer (625, Radiometer, Denmark). All parameters were kept stable during the entire scan session by adjusting respiration volume and giving saline drop.

After injection of 147 MBq **[^{123}I]-*S*-2** dynamic SPECT scanning was conducted over a period of 4 h (30 × 2 min in the first hour followed by 18 × 10 min). SPECT imaging was performed on a triple-head IRIX camera (Philips, Cleveland, USA) fitted with low-energy, general-all-purpose parallel holed collimators (LEGAP-PAR). The spatial resolution of the camera is approximately 8.5 mm at 10 cm distance to the camera head. To allow later correction for septal penetration and backscatter from high-energy photons, the signal was recorded in two separate energy windows. Window 1 was centered at 159 KeV, width 32 KeV, and window 2 was centered at 200 KeV, width 32 KeV. Each camera covered 120 degrees of the circular orbit. Scans were performed in a continuous mode with an angular step of 3 degrees and 40 steps. The acquisition matrix was 128 × 128 with a pixel size of 2.33 mm in both directions.

For reconstruction, the projection image files were converted to DICOM format in the scanner software (Odyssey 9.2B; Philips, Cleveland, USA) and exported to UNIX platforms for further processing by matlab routines developed at the NRU (Neurobiology Research Unit, Copenhagen, Denmark). In Matlab 6.5, the images were converted from DICOM to Analyse format. Before reconstructing the projection images, the raw data of the two energy windows were subtracted in sinogram space to perform correction for penetration and backscatter from high-energy photons. The number of counts in the high-energy window was multiplied by 1.1, the factor was determined by recording the two energy windows of a ^{123}I-source contained in 6 mm lead. Reconstruction was performed by using standard filtered back projection with a low pass 4th order Butterworth 3D post-filter with a cut-off frequency of 0.4 Nyquist and using

uniform attenuation correction with an attenuation coefficient of 0.10 cm^{-1}. The complete subtraction and reconstruction algorithm was carried out in Matlab 6.5. The resulting series of images were converted into a dynamic file and a summed image using all frames.

For calculating time-activity curves (TACs) from midbrain, frontal cortex and cerebellum, the summed image was co-registered to a pig brain MRI-based atlas[18] using the program Register, a tri-planer viewer developed at the Montreal Neurological Institute, McGill University, Canada. Registration was achieved by manually marking homologue anatomical positions in the two scans and minimizing the root mean square distance between the landmarks. Then, TACs from the ROIs were calculated as previously described.[19] To minimize statistical noise in the signal, the regions thalamus, diencephalon and mesencephalon were pooled to obtain a larger midbrain region.

Results

Radiochemistry

The radiosyntheses of **[^{125}I]-2** and **[^{125}I]-(*S*)-2** were performed in a one step reaction from the corresponding bromo precursors **1** and ***S*-1**, respectively (Scheme 1).

For each radioligand, the radioactive product was collected after 29.5–30.5 min in two separate HPLC runs. The bromo precursors **1** and ***S*-1** were eluted after 20.5–26 min. The iodinated products, **[^{125}I]-2** and **[^{125}I]-(*S*)-2**, were obtained in approximately 35% radiochemical yield. The radiochemical purity of the final product was >98% as determined by analytical HPLC and no precursor could be detected in the UV-trace of the HPLC chromatogram. The identity of the product was confirmed by co-elution with the reference substance **2** in each case. The purified product was evaporated and formulated in 50% EtOH. In this medium, **[^{125}I]-2** has proven to be stable for at least 2 months (>95% pure).

Log *P* value

The iodo derivative **2** has a calculated log *P* value of 5.2.

In vitro binding studies

From saturation experiments in rat membrane homogenates previously described in detail, [16] Scatchard plot analysis was performed. The Scatchard plot was linear indicating only one binding site and the K_d values (mean ± SEM) were 0.7 ± 0.06 nM and 0.52 ± 0.02 nM for the iodinated derivatives **[^{125}I]-2** and **[^{125}I]-(*S*)-2**, respectively.

Ex vivo brain distribution studies in rats

Between 1.25 and 1.95 MBq of **[^{125}I]-2** or **[^{125}I]-(*S*)-2** was intravenously injected in the tail vein of the rats. Rats receiving **[^{125}I]-2** were decapitated between 1 and 6 h after injection as indicated in Table 1. The radioligand penetrated the blood–brain barrier resulting in a brain uptake of 0.34% injected dose after 1 h. After decapitation, the brain regions of interest were

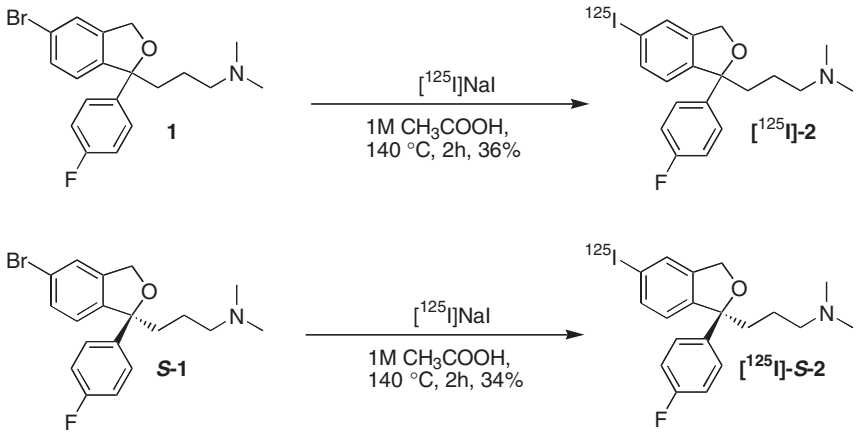

Scheme 1. Radiosynthesis of **[^{125}I]-2** and **[^{125}I]-(*S*)-2**.

Table 1. Regional brain distribution (% dose/g) in rat brain after intravenous injection of **[^{125}I]-2**

Brain region	1 h (n = 3)	2 h (n = 3)	3 h (n = 3)	4 h (n = 3)	6 h (n = 2)
Olfactory tuberli	0.18 ± 0.03	0.09 ± 0.02	0.08 ± 0.01	0.04 ± 0.01	0.03 ± 0.00
Hypothalamus	0.23 ± 0.03	0.12 ± 0.02	0.11 ± 0.02	0.05 ± 0.02	0.03 ± 0.00
Cerebellum	0.18 ± 0.03	0.08 ± 0.01	0.07 ± 0.01	0.03 ± 0.01	0.03 ± 0.00
Hippocampus	0.23 ± 0.04	0.12 ± 0.02	0.11 ± 0.20	0.04 ± 0.01	0.03 ± 0.01
Corpus striatum	0.23 ± 0.05	0.11 ± 0.02	0.09 ± 0.02	0.04 ± 0.01	0.03 ± 0.01
Thalamus	0.28 ± 0.04	0.17 ± 0.04	0.12 ± 0.02	0.05 ± 0.01	0.04 ± 0.01
Pre-frontal cortex	0.24 ± 0.04	0.11 ± 0.02	0.09 ± 0.01	0.04 ± 0.01	0.03 ± 0.00
Remaining cortex	0.23 ± 0.04	0.10 ± 0.02	0.09 ± 0.01	0.04 ± 0.01	0.03 ± 0.00

Values are mean ± SD.

dissected and weighted, and the radioactive content was counted and regional brain distributions (% dose/g) of compound **[^{125}I]-2** was determined (Table 1).

The maximal target-to-cerebellum ratios were found in the thalamus and hypothalamus regions after 2 h. Rats receiving **[^{125}I]**-(***S***)-**2** were decapitated after 2 h and the hypothalamus- and thalamus-to-cerebellum ratios were 2.1 and 2.4, respectively. In the blocking experiments, paroxetine (3 mg/kg) was injected in the tail vein of the rats ($n = 3$) 10 min prior to injection of **[^{125}I]-2**. After 2 h, the rats were decapitated and the thalamus- and hypothalamus-to-cerebellum ratios were significantly reduced (Figure 1).

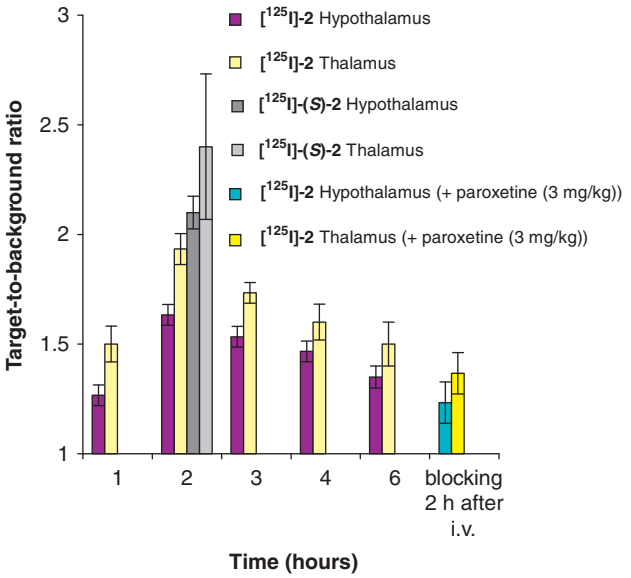

Figure 1. Thalamus- and hypothalamus-to-cerebellum ratios of **[^{125}I]-2** and **[^{125}I]-(*S*)-2** at different time points after intravenous injection. In the blocking experiments, the rats were sacrificed 2 h after injection. The values are mean ± SD.

SPECT study

[^{123}I]-(*S*)-2 was studied *in vivo* in the pig brain. Summed images and TACs from the midbrain, frontal cortex and cerebellum are shown in Figure 2. In this set-up, **[^{123}I]-(*S*)-2** peaks at around 20–40 min after injection. Uptake is highest in midbrain, slightly lower in frontal cortex and lowest in cerebellum. Target-to-cerebellar area under the curve (AUC) ratio is 1.20 for midbrain and 1.13 for frontal cortex.

Discussion

In our search for new SPECT tracers to study the SERT *in vivo*, we have synthesized the novel iodinated radioligands **[^{125}I]-2** and **[^{125}I]-(*S*)-2**, which are structurally related to the SSRI's citalopram and escitalopram. The iodo derivative **2** has a calculated log *P* of 5.2 and displays high affinity for the SERT and is highly selective as compared with the dopamine and noradrenaline transporter (Table 2).[20]

Table 2. Inhibition of [^{3}H]5-HT, [^{3}H]DA and [^{3}H]NA uptake for citalopram and iodo derivative **2**

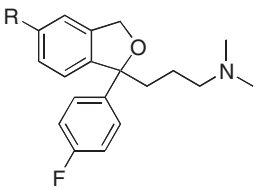

		Inhibition of [^{3}H]amine uptake, IC_{50} (nM)		
Compound	R	5-HT	DA	NA
Citalopram	CN	1.8	40 000	6100
2	I	3.5	2600	1300

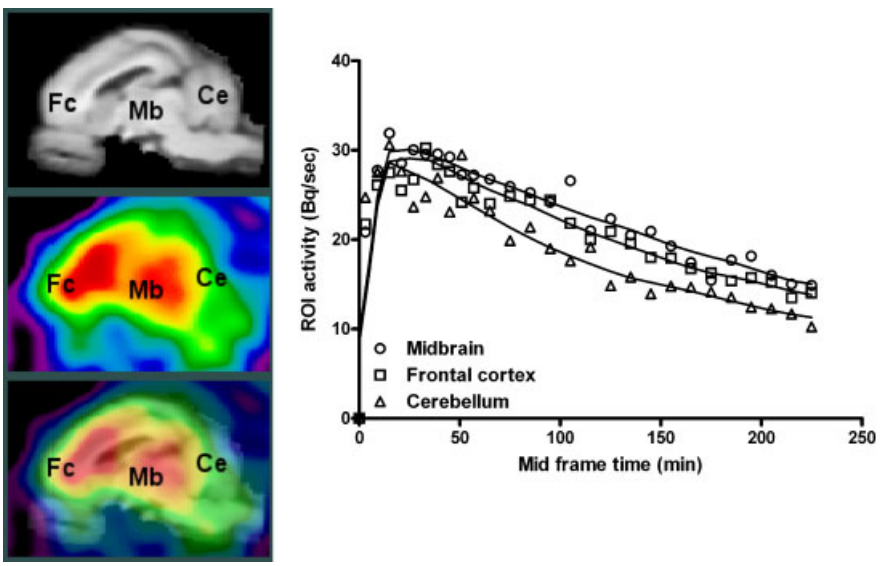

Figure 2. Summed SPECT images and TACs from the midbrain, frontal cortex and cerebellum of **[^{123}I]-(*S*)-(2)**.

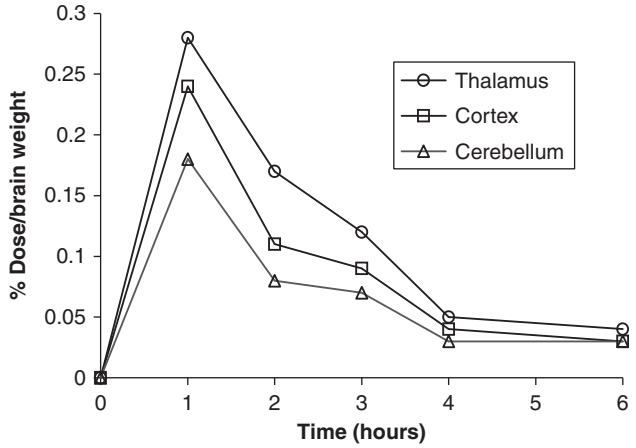

Figure 3. Regional brain distribution in the thalamus, cortex and cerebellum (% dose/g) in rat brain at various time points after intravenous injection of **[^{125}I]-2**. Values are mean, see also Table 1.

The radioligands **[^{125}I]-2** and **[^{125}I]-(*S*)-2** were synthesized from the corresponding bromo precursors **1** and ***S*-1,** respectively, in a Br/^{125}I exchange reaction[21] (Scheme 1). The radioiodinated products, **[^{125}I]-2** or **[^{125}I]-(*S*)-2**, were well separated from the bromo precursors **1** or ***S*-1**, respectively, under the HPLC conditions applied.

The K_d values of **[^{125}I]-2** (0.70 ± 0.06 nM) and **[^{125}I]-(*S*)-2** (0.52 ± 0.02 nM) are comparable with the values obtained for [^{3}H]citalopram ($K_d = 1$ nM)[22] and [^{3}H]escitalopram ($K_d = 0.71$ nM).[16] In *ex vivo* rat studies, **[^{125}I]-2** penetrated the blood–brain barrier (0.34% injected dose 1 h after injection) and the highest target-to-cerebellum ratios at all time points were found in the thalamus and hypothalamus. This corresponds well with the known high SERT densities in these regions of the brain.[23] Cerebellum, which has a low density of SERT sites, was used as reference region.[23] A maximal thalamus-to-cerebellum ratio of 1.9 was observed 2 h after intravenous injection of **[^{125}I]-2**. After pre-treatment with the SSRI paroxetine, the major parts of the specific binding in the thalamus and hypothalamus regions were reduced (Figure 1).

Since the established TAC indicated that a maximal ROI-to-cerebellum ratio was reached after 2 h this time point was used for further experiments with the biologically more active enantiomer, **[^{125}I]-(*S*)-2**.

Compared with **[^{125}I]-2** injection of **[^{125}I]-(*S*)-2** resulted, as expected, in an increased target-to-background ratio in *ex vivo* rat studies. The hypothalamus- and thalamus-to-cerebellum ratios were increased from 1.6 and 1.9 to 2.1 and 2.4, respectively (Figure 1).

The maximal uptake was reached after 1 h. The maximal target-to-cerebellum ratio reached after 2 h (Figure 3) was relatively fast compared with [^{125}I]ADAM,[24] which peaks after 4 h and slightly slower than [^{125}I]IDAM,[25] which peaks already after 60 min.

The target-to-cerebellum ratio was somewhat lower than [^{125}I]ADAM and [^{125}I]IDAM, where hypothalamus-to-cerebellum ratios are 5.0 and 2.8, respectively.[26]

TACs show that in the pig brain the uptake of **[^{123}I]-(*S*)-2** peaks at around 20–40 min after injection, slightly faster in transporter rich than in transporter poor regions. Uptake was higher in transporter rich regions as midbrain compared with cerebellum with very low densities of SERT. Target-to-cerebellar AUC ratio was 1.20 for the high-binding region midbrain. The TAC from the frontal cortex and the midbrain are almost overlapping, although a difference in SERT concentrations between the two regions is approximately 3.5, as measured with [^{11}C]DASB PET.[27] This can partly be ascribed to partial volume effects that are caused by the limited spatial resolution of SPECT. This leads to an underestimation of regional radioactivity distribution in regions with high radioactivity concentration relative to the surroundings, and also to the converse situation with overestimation in regions with low radioactivity concentration.[28] With a co-registered magnetic resonance image, it is possible to correct for these effects of partial volume.[29] Even when partial volume effects and the small volume of the pig brain (180 g) are taken into account, the TAC in the pig brain are considerably less promising than in our rat data. However, without a partial volume correction, we still detect a difference between high and low activity regions, and this difference is expected to be even higher in partial volume corrected data.

The low target-to-background ratio in the brain could either be due to too high non-specific binding or to too low specific binding. The estimated log *P* value of 5.2, which is considered to be relatively high, could result in slow washout of non-specific binding. We previously found that the non-specific binding of the carbon-11 labelled *S*-enantiomer of citalopram (log *P* 3.6) is also high in rats,[30,31] as it is in humans[30] and as well when a carbon-11 labelled citalopram derivative where the cyano group was changed to a methyl group (log *P* 4.6) was studied in non-human primates.[32]

It is also possible that the binding affinity of **[^{125}I]-(*S*)-2** (0.52 ± 0.02 nM) for SERT is too low. We have previously estimated that the imaging of SERT in a high-density region in the human brain requires radioligands with K_d values between 0.03 and 0.3 nM.[17] We do not know whether the binding affinity of **[^{125}I]-(*S*)-2** displays species differences in the rat and human brain. However, based on our previous experiments that included radiolabelled (+)McN5652, DASB, ADAM, MADAM, escitalopram, fluoxetine and paroxetine, only paroxetine displayed higher affinity for monkey SERT compared with rat SERT.[17] If **[^{125}I]-(*S*)-2** also has lower or equal affinity for the human SERT compared with the rat SERT, our finding supports the notion that successful SERT radioligands should have an affinity in the range given above.

Metabolic degradation of citalopram invariably occurs at the dimethyl amino group.[33] Assuming that the minor differences between the cynao- and iodo substituents present in citalopram and **2** do not play a role for the metabolic process, the two major radiometabolites of **[^{123}I]-(*S*)-2** would be either glucoronides or the desmethyl derivative. This is in accordance with our experience with *S*-[*N*-methyl-^{11}C]citalopram in non-human primates where we found indications of formation of polar metabolites only (unpublished data). Therefore, we do not expect the formation of lipophilic radiolabelled metabolites from **[^{123}I]-(*S*)-2**. Although glucoronides cannot cross the blood–brain barrier, we cannot exclude that a radiolabelled demethylated metabolite to some extent may also contribute to the insufficient target-to-background signal in pigs.

Conclusions

Our results indicate that despite its superior selectivity towards the SERT, **[^{123}I]-(*S*)-2** is not better SPECT radioligand than

[^{123}I]ADAM for SERT. It is difficult to predict the *in vivo* characteristics of a radioligand based on *in vitro* data alone. Studies in small animals such as rats can give good indications of the fate of the radioligand. However, for a series of radioligands with promising properties a conclusion should be based on an *in vivo* PET/SPECT study in larger animals such as non-human primates or pigs. Based on our data, [^{123}**I**]-(***S***)-**2** does not show a great potential as a SERT-radioligand for human SPECT studies.

Acknowledgements

This work is supported by The Centre for Drug Design and Transport through a grant from The Danish Medical Research Council. Anne Mette Dall and Inge Møller are gratefully acknowledged for excellent technical assistance.

References

[1] R. E. Henkin, M. A. Boles, G. L. Dillehat, J. R. Halama, S. M. Karesh, R. H. Wagner, A. M. Zimmer (Ed.), in *Nuclear Medicine*, Vol. 1, Mosby Year Book Inc., **1996**.
[2] M. B. Keller, *J. Clin. Psychiatry* **2001**, *61*, 896.
[3] A. A. Wilson, N. Ginovart, M. Schmidt, J. H. Meyer, P. G. Threlkeld, S. Houle, *J. Med. Chem.* **2000**, *43*, 3103.
[4] M. Ichise, J. S. Liow, J. Q. Lu, A. Takano, K. Model, H. Toyama, T. Suhara, K. Suzuki, R. B. Innis, R. E. Carson, *J. Cereb. Blood Flow Metab.* **2003**, *23*(9), 1096.
[5] J. Tarkiainen, J. Vercouillie, P. Emond, J. Sandell, J. Hiltunen, Y. Frangin, D. Guilloteau, C. Halldin, *J. Label. Compd. Radiopharm.* **2001**, *44*, 1013.
[6] J. Lundberg, I. Odano, H. Olsson, C. Halldin, L. Farde, *J. Nucl. Med.* **2005**, *46*(9), 1505.
[7] J. Jarkas, J. R. Votaw, R. J. Voll, L. Williams, V. M. Camp, M. J. Owens, D. C. Purselle, J. D. Brenner, C. D. Kilts, C. B. Nemeroff, M. M. Goodman, *Nucl. Med. Biol.* **2005**, *32*, 211.
[8] J. A. Nye, J. R. Votaw, J. Jarkas, D. C. Purselle, V. Camp, J. D. Brenner, C. D. Kilts, C. B. Nemeroff, M. M. Goodman, *J. Nucl. Med.* **2008**, *49*, 2018.
[9] P. D. Acton, M. Mu, K. Plössl, C. Hou, M. Siciliano, Z-P. Zhuang, S. Oya, S.-R. Choi, H. F. Kung, *Eur. J. Nucl. Med.* **1999**, *26*, 1359.
[10] P. D. Acton, M.-P. Kung, M. Mu, K. Plössl, C. Hou, M. Siciliano, S. Oya, H. F. Kung, *Eur. J. Nucl. Med.* **1999**, *26*, 854.
[11] P. D. Acton, S.-R. Choi, C. Hou, K. Plössl, H. F. Kung, *J. Nucl. Med.* **2001**, *42*, 1556.
[12] T. A. Kauppinen, K. A. Bergström, P. Heikman, J. Hiltunen, A. K. Ahonen, *Eur. J. Nucl. Med. Mol. Imaging* **2003**, *30*, 132.
[13] K. Erlandsson, T. Sivananthan, D. Lui, A. Spezzi, C. E. Townsend, S. Mu, R. Lucas, S. Warrington, P. J. Ell, *Eur. J. Nucl. Med. Mol. Imaging* **2005**, *32*, 1329.
[14] V. G. Frokjaer, L. H. Pinborg, J. Madsen, R. de Nijs, C. Svarer, A. Wagner, G. M. Knudsen, *J. Nucl. Med.* **2008**, *49*(2), 247.
[15] J. Madsen, P. Merachtsaki, P. Davoodpour, B. Bergström, B. Långström, K. Andersen, C. Thomsen, L. Martiny, G. Knudsen, *Bioorg. Med. Chem.* **2003**, *11*, 3447.
[16] B. Elfving, B. Björnholm, B. Ebert, G. M. Knudsen, *Synapse* **2001**, *41*, 203.
[17] B. Elfving, J. Madsen, G. M. Knudsen, *Synapse* **2007**, *61*(11), 882.
[18] H. Watanabe, F. Andersen, F. Simonsen, S. M. Evans, A. Gjedde, P. Cumming, *Neuroimage* **2001**, *14*(5), 1089.
[19] F. Andersen, H. Watanabe, C. Bjarkam, E. H. Danielsen, P. Cumming, *Brain. Res. Bull.* **2005**, *66*(1), 17.
[20] H. Lundbeck A/S, unpublished data.
[21] M. Ceusters, D. Tourwé, J. Callaerts, J. Mertens, A. Peter, *J. Org. Chem.* **1995**, *60*, 8324.
[22] P. Plenge, E. T. Mellerup, *J. Neurochem.* **1991**, *56*, 248.
[23] R. Cortés, E. Soriano, A. Pazos, A. Probst, J. M. Palacios, *Neuroscience* **1988**, *27*, 473.
[24] S. Oya, S.-R. Choi, C. Hou, M. Mu, M.-P. Kung, P. D. Acton, M. Siciliano, H. F. Kung, *Nucl. Med. Biol.* **2000**, *27*, 249.
[25] M.-P. Kung, C. Hou, S. Oya, M. Mu, P. D. Acton, H. F. Kung, *Eur. J. Nucl. Med.* **1999**, *26*, 844.
[26] S. Oya, S.-R. Choi, C. Hou, M. Mu, M.-P. Kung, P. D. Acton, M. Siciliano, H. F. Kung, *Nucl. Med. Biol.* **2000**, *27*, 249.
[27] S. B. Jensen, D. F. Smith, D. Bender, S. Jakobsen, D. Peters, E. Ø. Nielsen, G. M. Olsen, J. Scheel-Krüger, A Wilson, P. Cumming, *Synapse* **2003**, *49*(3), 170.
[28] E. J. Hoffman, S. C. Huang, M. E. Phelps, *J. Comput. Assist. Tomogr.* **1979**, *3*, 299.
[29] H. W. Muller-Gartner, J. M. Links, J. L. Prince, R. N. Bryan, E. McVeigh, J. P. Leal, C. Davatzikos, J. J. Frost, *J. Cereb. Blood Flow Metab.* **1992**, *12*, 571–583.
[30] S. P. Hume, A. A. Lammertsma, C. J. Bench, V. W. Pike, C. Pascall, R. J. Dolan, *Int. J. Rad. Appl. Instrum. B.* **1992**, *19*(8), 851.
[31] J. Madsen, B. Elfving, K. Andersen, L. Martiny, G. M. Knudsen, *J. Label. Compd. Radiopharm.* **2004**, *47*, 335.
[32] J. Madsen, P. Merachtsaki, P. Davoodpour, M. Bergström, B. Långström, K. Andersen, C. Thomsen, L. Martiny, G. M. Knudsen, *Bioorg. Med. Chem.* **2003**, *11*, 3447.
[33] L. Dalgaard, C. Larsen, *Xenobiotica* **1999**, *29*(10), 1033.